WAVES AND NEGATIVE REFRACTION IN MAGNETIZED PLASMA WITH FERRITE GRAINS

By

MARKOS MEHRETIE

SUBMITTED IN PARTIAL FULFILLMENT OF THE
REQUIREMENTS FOR THE DEGREE OF
MASTER OF SCIENCE IN PHYSICS
AT
ADDIS ABABA UNIVERSITY
ADDIS ABABA, ETHIOPIA
JUNE 2012

ADDIS ABABA UNIVERSITY

DEPARTMENT OF

PHYSICS

Supervisor: _____

Prof.V.N.Mal'nev

Examiners: _____

Dr. Mulugeta Bekele

_____

Prof. p.Singh

ADDIS ABABA UNIVERSITY

Date: **June 2012**

Author: **MARKOS MEHRETIE**

Title: **WAVES AND NEGATIVE REFRACTION IN MAGNETIZED PLASMA WITH FERRITE GRAINS**

Department: **Physics**

Degree: **M.Sc.** Convocation: **June** Year: **2012**

Permission is herewith granted to Addis Ababa University to circulate and to have copied for non-commercial purposes, at its discretion, the above title upon the request of individuals or institutions.

Signature of Author

Table of Contents

List of Figures

Abstract

This thesis describes that some electrodynamical properties of left-handed media and experiments realize to allow these metamaterials. The dispersion properties of a material is controlled by both dilectric permittivity and magnetic permeability tensors. The dispersion of the permittivity is caused by electron-ion plasma and the dispersion of permeability is caused by the high frequency magnetization of the ferromagnetic grains. The propagation of high frequency EMWs in the low temperature magnetized plasma with ferromagnetic grains (MPFG) is analyzed. Our MPFG system becomes transparent for the waves that cannot propagate in conventional magnetized plasma, which is the dispersion of permeability is zero. It is shown that the refractive index of the extraordinary wave propagating along the external magnetic field through MPFG can be negative and the phase velocity also negative in the vicinity of ω_c. The strong dispersion of the refractive index and the group velocity results in the spreading of the wave packets, which propagate with velocity much smaller than the speed of light.

Acknowledgements

I would like to express my sincere gratitude to my advisor Prof. Mal'nev for his unlimited and constractive guidance, suggestion and comment during my work. I am grateful to all my families for thier effort and encouraging me to do my work specially my brothers Solomon Mehretie and Amare Mehretie for their accadamic and financial supports.

I am also thankful to Belayneh Mesfin for his support in giving materials and his constractive guidance.

Chapter 1

Introduction

In this historical overview, we see that the developments of understanding of the phenomenon of "negative refraction". The earliest idea on negative refraction came by Prof.L.I.Mandelshtan (1879-1944) from Moscow university. He noticed that since the phase velocity does not have to have the same direction as the power flow vector, "negative refraction" is possible[1]. Materials with negative parameters as backward-wave materials were mentioned by D.V.Sivukhin in 1957. He noticed that media with negative parameters are backward-wave media, but had to state that media with $\varepsilon < 0$ and $\mu < 0$ are not known[2].

An important step was made by V.G.Veselago in 1967. Prof.Veselago made a systematic study of electromagnetic properties of materials with negative parameters and reported on his unsuccessful search for such media. He published his article about the theoretical properties of media that can be effectively be said to possess both negative permittivity and negative permeability with in a certain frequency range[3]. The dielectric constant ε and the magnetic permeability μ are the fundamental characteristic quantities which determine completely the peculiarities of propagation of electromagnetic waves in matter. For the last two decades, many scientists are concerned about the theoretical and experimental studies of physical properties of the so called left-handed media (LHM) or media with a negative refraction index (NRM). May be it is important to remind that, the ordinary right-handed media(RHM), the Poynting vector $\vec{S}$, and the wave vector $\vec{K}$

have the same direction. This means that the phase velocity of a wave in RHM and its group velocity have the same direction. But in the case of LHM the phase velocity of electromagnetic wave has opposite direction from group velocity.

As we mentioned earlier, Veselago studied theoretically optical properties of the media with negative dielectric permittivity ε and magnetic permeability μ simultaneously and showed that they can be described phenomenologically with the help of a negative refraction index $\eta = -\sqrt{(-\varepsilon(\omega))(-\mu(\omega))}$[2].

The main problem on the way of experimental realizations of LHM is to find the frequency ranges where $\varepsilon(\omega)$ and $\mu(\omega)$ can be negative simultaneously. Basically, a realization of this condition is limited by the dispersion properties of the magnetic permeability. The point is that $\mu(\omega)$ practically equals to unity in natural substances at frequencies much lower than the optical one.

Pendry with colleagues considered the electrodynamic properties of a lattice of wires (a low frequency plasma medium with negative permittivity at frequencies lower than the plasma frequency) and split ring resonators (a medium with negative permeability) and showed that this system can be treated as LHM in some comparatively narrow super high-frequency(SHF) range. His popular approach describes a slab of a hypothetical material with a negative refraction index would exponentially amplify the evanescent waves, thus allowing perfect imaging of all optical fields[4,5]. However, such materials do not exist in nature and therefore artificial structures are required. The recent publication demonstrates experimentally that materials with anomalous magneto-resistance like $La_{\frac{2}{3}}Ca_{\frac{1}{3}}M_nO_3$ possess the negative refraction in the GH_z range[4].

In this thesis, we study the peculiar properties associated with the ordinary and extraordinary super high frequency (SHM) waves in Magnetized plasma with ferrite grains(MPFG). In this system the dispersion properties controlled by the permittivity $\tilde{\varepsilon}$ and permeability $\tilde{\mu}$ tensors simultaneously can be obtained in the laboratory by adding ferrite (ferromagnetic) grains to magnetized electron-ion plasma(we call it MPFG). In a narrow frequency

band around the electron cyclotron frequency ω_c, the dispersion of the permittivity $\tilde{\varepsilon}$ and permeability $\tilde{\mu}$ tensors may considerably change the refractive index, phase, and group velocities of these waves compared to the conventional magnetized plasma(CMP)[6,7,8].

The rest of the thesis is designed as follows. In Chapter two, some electro-dynamical properties of left-handed media briefly described. In Chapter three, the building blocks ofleft-handed media, Arrays of Long Metallic Wires (ALMWs) and Split-Ring Resonators (SRR) are discussed. In Chapter four, the permeability tensor of ferromagnetic grains and permittivity tensor of magnetized electron-ion plasma are calculated. In Chapter five, the equation of the refractive index of MPFG is derived and the frequency range where it becomes negative is analyzed. Also the phase and group velocities of the extraordinary wave through MPFG is calculated. In Chapter six, the work of thesis concluded.

Chapter 2

Electrodynamics of Left-Handed Media(LHM)

Metamaterials are artificially constructed, having electromagnetic properties not generally found in nature. In particular, metamaterials created by arrays of wires and split-ring resonators can possess a negative real part of magnetic permeability and dielectric permittivity for microwaves. These materials are referred to as left-handed materials(LHM). Media with negative permittivity ($\varepsilon < 0$) can be found in nature. The best known examples are low-loss plasmas, and metals and semiconductors at optical and infrared frequencies (sometimes called solid-state plasmas). Media with negative μ are less common in nature due to the weak magnetic interactions in most solid-state materials. Only in ferromagnetic materials are magnetic interactions strong enough to produce regions of negative magnetic permeability. The electrodynamics of media with simultaneously negative ε and μ was discussed and analyzed by Professor Veselago[3].

2.1 Wave Propagation in Left-Handed Media

In order to show wave propagation in left-handed media, we will first reduce Maxwell's equation to the wave equation.

$$\left(\nabla^2 - \frac{\eta^2}{c^2}\frac{\partial^2}{\partial t^2}\right)\psi = 0, \tag{2.1.1}$$

where η is the refractive index, c is the velocity of light in vacuum and $\frac{\eta^2}{c^2} = \varepsilon\mu$. As the

squared refractive index η^2 is not affected by a simultaneous change of sign in ε and μ, it is clear that low-loss left-handed media must be transparent. In view of the above equation, we can obtain the impression that solutions to Equation (2.1.1) will remain unchanged after a simultaneous change of the signs of ε and μ. However, when Maxwell's first-order differential equations are explicitly considered,

$$\vec{\nabla} X \vec{E} = -i\frac{\omega}{c}\mu\vec{H} \tag{2.1.2}$$

$$\vec{\nabla} X \vec{H} = i\frac{\omega}{c}\varepsilon\vec{E} \tag{2.1.3}$$

it becomes apparent that these solutions are quite different. In fact, for plane-wave fields of the kind $\vec{E} = \vec{E_0} exp(i(\vec{k}\cdot\vec{r} - \omega t))$ and $\vec{H} = \vec{H_0} exp(i(\vec{k}\cdot\vec{r} - \omega t))$, the above equations reduce to

$$\vec{k} X \vec{E} = \frac{\omega}{c}\tilde{\mu}\cdot\vec{H} \tag{2.1.4}$$

$$\vec{k} X \vec{H} = -\frac{\omega}{c}\tilde{\varepsilon}\cdot\vec{E} \tag{2.1.5}$$

where $\tilde{\varepsilon}$ and $\tilde{\mu}$ are permittivity and permeability tensors, and showing that $\vec{E}$, $\vec{H}$ and $\vec{k}$ now form a left-handed triplet, as illustrated in Figure (2.1). In fact, this result is the original reason for the denomination of negative $\tilde{\varepsilon}$ and $\tilde{\mu}$ media as "left-handed" media[3].

The main physical implication of the aforementioned analysis is backward-wave propagation. In fact, the direction of the time-averaged flux of energy is determined by the real part of the Poynting vector$\vec{S}$,

$$\vec{S} = \frac{c}{8\pi} Re(\vec{E} X \vec{H^*}) \tag{2.1.6}$$

which is unaffected by a simultaneous change of sign of $\tilde{\varepsilon}$ and $\tilde{\mu}$. Thus $\vec{E}$,$\vec{H}$, and $\vec{S}$ still form a right-handed triplet in a left-handed medium. Therefore, in such media, energy and wavefronts travel in opposite directions (backward propagation).

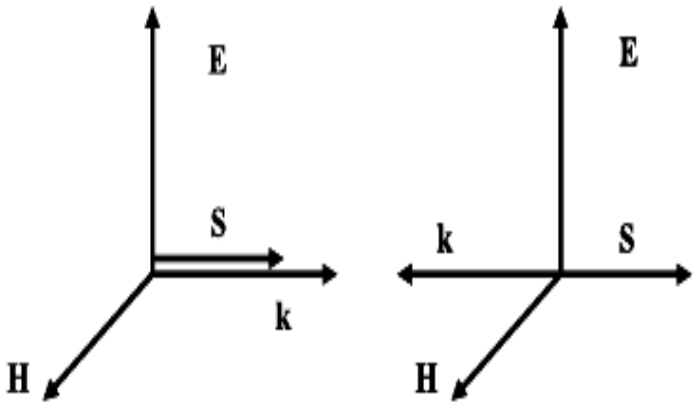

Figure 2.1: Illustration of the system of vectors $\vec{E}, \vec{H}, \vec{k}$, and $\vec{S}$ for a plane transverse electromagnetic (TEM) wave in an ordinary (left) and left-handed (right) medium.

2.2 Negative Refraction

Let us now consider the refraction of an incident optical ray at the interface between ordinary ($\varepsilon > 0$ and $\mu > 0$) and left-handed media ($\varepsilon < 0$ and $\mu < 0$). Boundary conditions impose continuity of the tangential components of the wave vector along the interface. Thus from the aforesaid backward propagation in the left-handed region, it immediately follows that, unlike in ordinary refraction, the angles of incidence and refraction must have opposite signs. This effect is illustrated in Figure (2.2). From the aforementioned continuity of the tangential components of the wave-vectors of the incident θ and refractedθ_2 rays,

$$\frac{sin\theta_i}{sin\theta_r} = \frac{-k_2}{k_1} = \frac{\eta_2}{\eta_1} < 0 \tag{2.2.1}$$

which is the well-known Snell's law. In this expression, η_1 and η_2 are the refractive indicies of the the ordinary and left-handed media, respectively. Assuming $\eta_1 > 0$, from Equation (2.2.1) it follows that $\eta_2 < 0$. That is, the sign of the square root in the refractive index definition must be chosen to be negative

$$\eta = -c\sqrt{\varepsilon\mu} < 0 \tag{2.2.2}$$

For this reason, left-handed media are also referred to as negative refractive index or

negative refractive media.

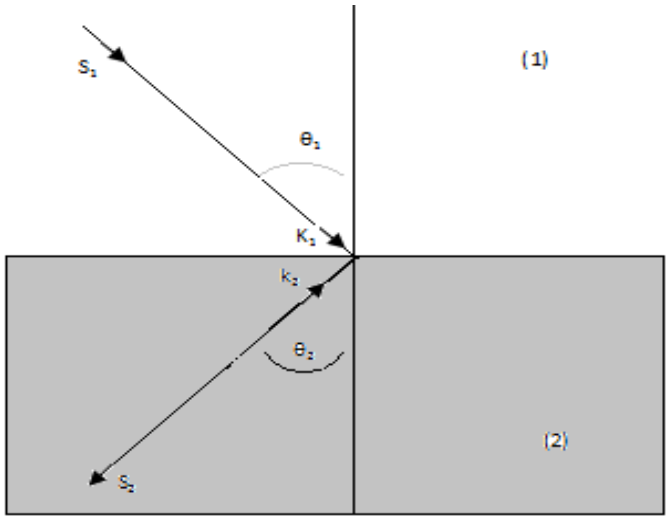

Figure 2.2: Graphic demonstration of the negative refraction between ordinary (1) and left-handed (2) media.

2.3 Fermat's Principle

Fermat's principle is a concise statement that contains all the physical laws, such as the law of reflection and the law refraction, in geometrical optics. Fermat's principle states that the path of a light ray follows an extremum in comparison with the nearby paths.

According to Fermat's principle, out of the many paths that connect the two points

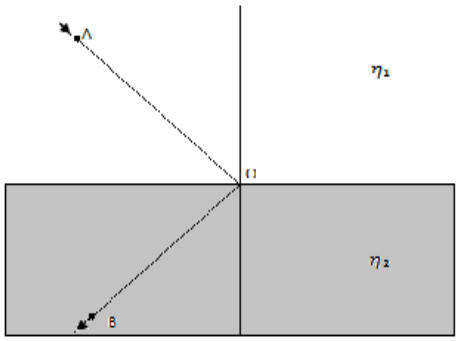

Figure 2.3: The refraction of light in left-handed media

A and B in Figure (2.2), the light ray would follow that path for which the optical path length L between the two points is an extremum[9].$i.e, L = \eta_1(AO) + \eta_2(OB)$

$$\delta L = \delta \int_A^B \eta dl = 0 \tag{2.3.1}$$

in which δ represents a small variation.

If the index of refraction is changed from point to point, the optical length L between points A and B will be:

$$L = \int_A^B \eta dl \tag{2.3.2}$$

Since our medium has negative refractive index ($\eta < 0$), the optical length L can have negative value or probably null for special cases. It also becomes apparent that the time taken by light to travel between two points is not related to the optical length through the usual formula for ordinary weakly dispersive media, that is $t = \frac{L}{c}$. Therefore, the path followed by light in optical systems containing left-handed media is not necessarily the shortest in time. From Equation $L(2.3.2)$, it follows that the optical length between two points, A and B, on a given optical ray is proportional to the phase advance between such points: $\Delta\phi = -K\overline{AB} = -\eta(\frac{\omega}{c})\overline{AB} = -(\frac{-\omega}{c})L$.

2.4 Inverse-Doppler Effect

When a moving receiver detects the radiation coming from a source at rest in a uniform medium, the detected frequency of the radiation depends on the relative velocity of the emitter and the receiver. This is the well-known Doppler effect. If this relative velocity is much smaller than the velocity of light, a non relativistic analysis suffices to describe such an effect. If the receiver moves towards the source wavefronts and receiver move in opposite directions. Therefore, the frequency seen by the receiver will be higher than the frequency measured by an observer at rest. However, if the medium is a left-handed

material, wave propagation is backward, and wavefronts move towards the source. Therefore, both the receiver and the wavefronts move in the same direction, and the frequency measured at the receiver is smaller than the frequency measured by an observer at rest. A straight forward calculation shows that the aforementioned frequency shifts are given by

$$\Delta\omega = \stackrel{+}{-}\omega_0 \frac{\upsilon}{\upsilon_p} \tag{2.4.1}$$

where ω_0 is the frequency of the radiation emitted by the source, υ is the velocity at which the receiver moves towards the source, υ_p the phase velocity of light in the medium, and the $\stackrel{+}{-}$ sign applies to ordinary/left-handed media. Equation (2.4.1) can be written in a more compact form as

$$\Delta\omega = \omega_0 \frac{\eta\upsilon}{c} \tag{2.4.2}$$

where η is the refractive index of the medium and c the velocity of light in free space. In Equation (2.4.2), $\Delta\omega$ is the difference between the frequency detected at the receiver and the frequency of the oscillation of the source. For $\eta < 0$, the frequency shift becomes negative for positive υ(receiver moving towards the source), the group velocity $\frac{d\omega}{dk}$ in left-handed media, a negative frequency shift results in an increase of K. Therefore, a shift towards shorter wavelengths is seen when the receiver approaches the source, both in ordinary and left-handed media.

2.5 Cerenkov Radiation

Cerenkov radiation occurs when a charged particle enters an ordinary medium at a velocity higher than the velocity of light in such a medium. If the deceleration of this particle is not too high, its velocity can be considered approximately constant over many wave periods. As a charged particle travels, it disrupts the local electromagnetic field (EM) in its medium. Electrons in the atoms of the medium will be displaced, and the

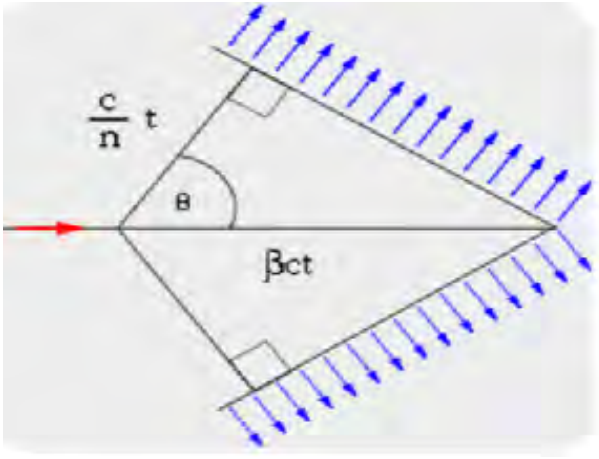

Figure 2.4: Schematic of Cerenkov radiation in conventional material medium with positive refractive index.

atoms become polarized by the passing EM field of a charged particle. Photons are emitted as an insulator's electrons restore themselves to equilibrium after the disruption has passed. In normal circumstances, these photons destructively interfere with each other and no radiation is detected. However, when a disruption which travels faster than light is propagating through the medium, the photons constructively interfere and intensify the observed radiation.

In the Figure(2.4), the particle travels in a medium with speed υ_p and we define the ratio between the speed of the particle and the speed of light as $\beta = \frac{\upsilon_p}{c}$. If η is the refractive index of the medium, then the emitted light waves travel at speed $\upsilon_{em} = \frac{c}{\eta}$. In the given time t, the particle travels the distance

$$X_p = \upsilon_p t = \beta c t \tag{2.5.1}$$

whereas the emitted electromagnetic waves are constricted to travel the distance

$$X_{em} = \upsilon_{em} t = \frac{c}{\eta} t \tag{2.5.2}$$

so

$$cos\theta = \frac{1}{\eta\beta} = \frac{c}{\eta v} \tag{2.5.3}$$

Note that since this ratio is independent of time, one can take arbitrary lines and achieve similar triangles. The angle stays the same, meaning that subsequent waves generated between the initial time $t = 0$ and final time t will form similar triangles with coinciding right end points to the one shown.

One more effect, whose realization greatly depends on simultaneous change of the signs of ε and μ, is the Cerenkov effect. As described above the angle of the radiated conical wavefront is given by the velocity of the particle v with respect to the phase velocity of EM waves v_{ph} within the medium in the following manner:

$$cos\theta = \frac{v_{ph}}{v} = \frac{\frac{c}{n}}{v} \tag{2.5.4}$$

where θ is the angle between the particle velocity and the radiated EM wavefront. It is clear from the logic of the above derivation that the conclusion on the direction of the emission tacitly assumed that the group velocity v_{gr} corresponding to the wave vector $\vec{K}$ was positive, that is directed along $\vec{S}$. But if the phase velocity is negative ,i.e, directed opposite to $\vec{S}$, radiation will be directed backward rather than forward as in the case of ordinary material (RHM). Therefore if the index of refractions become negative, it is obvious that angle lies in the second quadrant, and here under, the cone of the Cerenkov radiation is directed back.

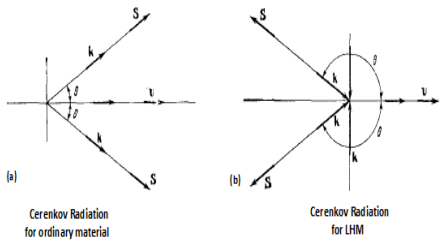

Figure 2.5: Schematic of backward Cerenkov radiation in a left-handed medium, showing the reverse cone.

Chapter 3

Different Experimental Realizations of Left-Handed Media

Different experiments have done by many scientists to overcome metamaterials with simultaneous negative dielectric permittivity and negative magnetic permeability. In 2001, Smith and his team in San Diego demonstrated the first artificially fabricated metamaterial that has the peculiar property of left-handed materials: it bends electromagnetic waves in the opposite direction to normal materials. This metamaterial is composed of a periodic arrangement of metallic printed lines or rods that exhibit a negative permittivity, and split ring resonators that exhibit a negative permeability[4,5,10]. Therefore, such composite structure exhibits a simultaneously negative permittivity and negative permeability and represents an example of Veselago's left-handed materials.

To understand how the metamaterial function, it is best to follow the historical steps that lead to the current geometry. First, it was shown that a three- dimensional array of thin, continuous (very long) metal wires exhibit a resonant frequency response similar to that of a plasma medium. At frequencies below the resonant plasma frequency, the electric permittivity becomes negative, the wave vector is imaginary, and there is no transmission. Above the plasma frequency, the permittivity is real and transmission occurs. Secondly it was demonstrated that negative magnetic permeability could be achieved using an array of split ring resonators. Close to resonance, the resonators produce strong magnetic field

in the directions opposite to the incident magnetic fields resulting a negative effective permeability.

3.1 Arrays of Long Metallic Wires(ALMWs)

A periodic array of metallic thin wires are commonly utilized to obtain negative permittivity ($\varepsilon < 0$) in the microwave spectrum. The real part of permittivity parameter of a plasma medium is negative permittivity under a specific frequency called plasma frequency. In visible light and ultraviolet light frequencies, negative dielectric permittivity is dominant for metals as a result of the plasma frequency of metals which is seen in optical frequencies. However, it is hard to have negative dielectric permittivity at lower frequencies, such as near infrared and the microwave regime; because, the dissipation dominates in metallic media as a result of significant increase in the dissipation of the the plasmon's energy. Therefore, the dielectric permittivity becomes purely imaginary.

In 1996, Pendry and others proposed the arrangement of periodic metal wires for the dispersion of the plasma frequency into the near infrared and GHz band. The physical mechanism behind Pendry et al.'s suggestion is the confinement of electrons into thin wires for enhancing the effective electron mass through self-inductance[5]. From the Drude-Lorentz atomic model

$$\varepsilon_{eff} = 1 - \frac{\omega_p^2}{\omega^2 - \omega_0^2 + i\Gamma\omega} \tag{3.1.1}$$

where ω_p is the plasma frequency, ω_0 is the resonant frequency and Γ is damping factor, which is approximately zero in our case. The free electron contribution in metals corresponds to ω_0=0. Therefore, the proposed structure has negative permittivity at microwave frequencies by using suitable parameters.

$$\varepsilon_{eff} = 1 - \frac{\omega_p^2}{\omega^2} \tag{3.1.2}$$

From classical formula of plasma frequency

$$\omega_p^2 = \frac{n_{eff} \cdot e^2}{\varepsilon_0 \cdot m_{eff}}$$

we can get the effective dielectric permittivity.

A structure which behaves just like a low density plasma of very heavy charged particles is shown in Figure (3.1)[5].

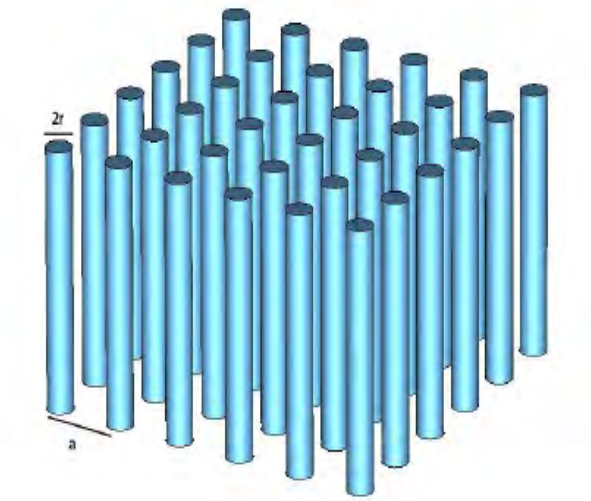

Figure 3.1: The schematic representation of a periodic metallic wire array. a is the lattice constant and r is radius of a single wire.

It consists of a three-dimensional lattice of very thin wires. In order to obtain the desired reduction in ω_p, we first consider a displacement of the electrons in the wires along one of the cubic axes. Therefore, only the wires directed along that axis are active and thus provide a lower effective density of electrons, n_{eff}, given by the area occupied by the active wires. Thus

$$n_{eff} = \frac{n\pi r^2}{a^2} \tag{3.1.3}$$

An even more proposed effect of constraining the electrons to run along thin wires is a result of the induced magnetic field which wraps the wires as the electrons are in motion. Suppose a current I flows in the wires. The magnetic field is

$$H(\rho) = \frac{I}{2\pi\rho} = \frac{nr^2ve}{2\rho} \tag{3.1.4}$$

Where ρ is the arbitrary distance from the wire and we have also expressed the current in terms of the electron velocity, v and the charge density ne. As we know, the magnetic field in terms of magnetic vector potential is

$$H(\rho) = \frac{1}{\mu_0}\nabla X A(\rho) \tag{3.1.5}$$

where $A(\rho) = \frac{\mu_0 r^2 nve}{2} ln(\frac{a}{r})$. The importance of the divergence of the magnetic field with the wire radius as seen in Equation (3.1.3) is the contribution to the electronic momentum given by eA. We can view this contribution as defining a new effective mass for the electrons given by.

$$m_{eff} = \frac{\mu_0 e^2 n}{2\pi} ln(\frac{a}{r}) \tag{3.1.6}$$

Now we are in a position to obtain the reduced plasma frequency for the system:

$$\omega_p^2 = \frac{n_{eff} \cdot e^2}{\varepsilon_0 \cdot m_{eff}} = \frac{2\pi c^2}{a^2 ln(\frac{a}{r})} \tag{3.1.7}$$

Therefore, below this reduced plasma frequency we can obtain the negative permittivity.

3.2 Split-Ring Resonators (SRRs)

Because of the lack of magnetic charge analogous to an electric charge, it is more difficult to obtain a material with negative magnetic permeability. To obtain negative permeability, one has to extend the magnetic properties of the materials. In 1999, Pendry et al. introduced several configurations of conducting scattering elements displaying a magnetic response to an applied electromagnetic field when grouped into an interacting periodic array.

The periodic thin wire array that was mentioned in the previous section responds to an incident electromagnetic field such that the effective dielectric permittivity of the structure becomes negative below the plasma frequency, but its permeability remains positive. Since, a magnetic dipole moment can be created by a current carrying conductor loop; a metallic ring structure provides a suitable structure to obtain a strong magnetic response. However, the rings should also have capacitive elements such as splits in order to

be resonant at wavelengths much larger than diameter of the rings. One of the structures proposed by Pendry et al. is shown in Figure (3.2).

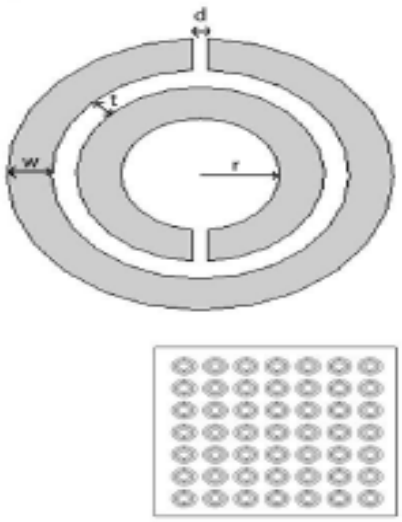

Figure 3.2: The split-ring structure: the capacitance across the ring causes to be the resonant

This structure for having negative permeability is a Split-Ring Resonator (SRR) structure, which is composed of two conducting rings with splits where the split locations are 180 degrees apart from each other. The splits are used to make the SRR resonant at wavelength much larger than the diameter of the SRR. The purpose of the second split-ring, inside and whose split is oriented oppositely to the outside split, is to generate a large capacitance in the small gap region. If the largest dimension of the SRR is much smaller than the wavelength of the resonance frequency, the response of a periodic arrangement of the SRR array can be analyzed by the permeability (μ_{eff}) can be used to define the permeability parameter of the resulting medium. The critical frequencies and effective permeability (μ_{eff}) for the SRR structure are analytically derived from the Drude-Lorentz atomic model[4,5]:

$$\mu_{eff}(\omega) = 1 - \frac{\omega_{mp}^2}{\omega^2 - \omega_{0m}^2 + i\Gamma\omega} \tag{3.2.1}$$

where

$$\omega_{mp} = \sqrt{\frac{3dc^2}{(1 - \frac{\pi r^2}{a^2})\pi^2 r^3}}, \quad \omega_0 = \sqrt{\frac{3dc^2}{\pi^2 r^3}} \tag{3.2.2}$$

Therefore, the effective magnetic permeability will be:

$$\mu_{eff} = 1 - \frac{\frac{\pi r^2}{a^2}}{1 + \frac{2\sigma j}{\omega r \mu_0} - \frac{3dc^2}{\pi^2 r^3 \omega^2}} \tag{3.2.3}$$

where, c is the speed of light in vacuum, a is the lattice constant for a unit cell, μ_0 is the magnetic permeability constant of vacuum, r is the radius of the inner ring and σ is the conductivity of the cylinder surface per unit area. The capacitance introduced into the system by the splits and the gap between the rings collaborates with the inductance introduced into the system by the metallic rings in order to resonate.

Chapter 4

Permeability and Permittivity Tensors of MPFG

4.1 Permeability Tensor of MPFG

Let us consider low temperature plasma with impurity of identical, spherical, micron ferrite grains, for example Yttrium iron garnet(YIG) of radius a and density number N_g in a constant magnetic field $\vec{H}_0$. The grain subsystem brings the dispersion of the permeability into conventional magnetized plasma (CMP) that is described by the permeability tensor $\tilde{\mu}$[6].

Before delving into the theory of the permeability tensor in ferrites, it is imperative that we say a few words about magnetization which goes to the heart of electrical modulation of magnetic property. If a ferromagnetic material were to be strained by applying a suitable stress along a crystal direction, the inter atomic distance along this direction as well as those along the other two orthogonal direction would change. Consequently the exchange interaction of the atomic spins would change, thereby changing magnetization of the ferromagnetic material. The converse is also true in that if a magnetic field is applied, the inter atomic distance would change[11].

To understand the ferromagnetic resonance (FMR) one should first consider the torque exerted on a magnetic dipole by the magnetic field $\vec{H}$. The torque is expressed by

$$\tau = \mu_0 \vec{m} X \vec{H} = -\mu_0 \gamma s X \vec{H} \tag{4.1.1}$$

where μ_0 is the permeability of a vacuum, s is the spin angular momentum that is opposite to the dipole magnetic moment m for the electron, and $\gamma = \frac{-m}{s}$ is the gyro-magnetic ratio.

The torque τ acting on a material is equal to the rate of change of angular momentum of the body.

$$\tau = \frac{ds}{dt} = -\frac{1}{\gamma}\frac{dm}{dt} = \mu_0 \vec{m} X \vec{H} \tag{4.1.2}$$

Under a strong enough static magnetic field, the magnetization of the material is assumed to be saturated and the total magnetization vector is given by $M = N_g m$, where N_g is the effective number of dipoles per unit volume. We can then obtain the macroscopic equation of motion of the magnetization vector from Equation (4.1.2) as:

$$\frac{dM}{dt} = -\mu_0 \gamma M X H \tag{4.1.3}$$

The minus sign is due to the negative charge of the electron that is carried out from γ. In many cases the absolute value of the electronic charge is used for practical purposes and the minus sign is removed. H is the vector sum of all fields external and internal, acting up on the magnetization and includes the DC field H_i and the RF field H_{ac}. H_i is the vector sum of all DC fields with in the material including that due to the externally applied DC field H_0 and any time-independent internal fields.

The total magnetic field can be expressed as:

$$H = H_0 + H_{ac} \tag{4.1.4}$$

The resulting magnetization will then have the form

$$M = M_s + M_{ac} \tag{4.1.5}$$

where M_s is the DC saturation magnetization and M_{ac} is the AC magnetization. In Equation(4.1.5), we have assumed that the H field is strong enough to drive the magnetization into saturation, which is true for practical application. The DC equation can be obtained from Equation(4.1.3) by neglecting all the AC terms.

$$\mu_0 \gamma M_s X H_0 = 0 \tag{4.1.6}$$

which indicates that, to the first order, the internal DC field and the magnetization are in the same direction.

Substituting Equation(4.1.4) and Equation(4.1.5) into Equation(4.1.3) and taking into account $\frac{dM_s}{dt} = 0$, we obtain

$$\frac{dM_{ac}}{dt} = \mu_0\gamma(M_s X H_{ac} + M_{ac} X H_0)$$

Further assuming that the AC field, and therefore the AC magnetization, have a harmonic time dependence, $e^{i\omega t}$, and by arbitrarily choosing the applied DC field direction along the z-axis, $\vec{H}_0\hat{z}$

$$\frac{dM_{ac}}{dt} = \mu_0\gamma(M_s H_y\hat{i} - M_s H_x\hat{j} + H_0 M_y\hat{i} - H_0 M_x\hat{j})$$

$$\Longrightarrow \frac{dM_{ac}}{dt} = \mu_0\gamma[(M_s H_y\hat{i} + H_0 M_y\hat{i} - (M_s H_x + H_0 M_x)\hat{j}]$$

$$\begin{cases} \omega M_x = \mu_0\gamma(-M_s H_y + H_0 M_y) \\ i\omega M_x = \mu_0\gamma(H_0 M_y - M_s H_y) \end{cases}$$

$$i\omega M_x = \omega_c M_y - \omega_m H_y \tag{4.1.7}$$

where $\omega_c = \mu_0\gamma H_0$, $\omega_m = \mu_0\gamma M_s$

And

$$\frac{dM_{acy}}{dt} = \mu_0\gamma(-H_0 M_x\hat{j} + M_s H_x\hat{j})$$

$$i\omega M_y = -\omega_c M_x + \omega_m H_x \tag{4.1.8}$$

solving Equation(4.1.7) and Equation(4.1.8) of M_x and M_y gives

$$M_x = \frac{\omega_c\omega_m}{\omega_c^2 - \omega^2} H_x + i\frac{\omega\omega_m}{\omega_c^2 - \omega^2} H_y \tag{4.1.9}$$

and

$$M_y = i\frac{\omega\omega_m}{\omega_c^2 - \omega^2} H_x + \frac{\omega_c\omega_m}{\omega_c^2 - \omega^2} H_y \tag{4.1.10}$$

These solutions can be written in tensor form

$$M_{ac} = \tilde{\chi} H_{ac} = \begin{pmatrix} \chi_{xx} & \chi_{xy} & 0 \\ \chi_{yx} & \chi_{yy} & 0 \\ 0 & 0 & 0 \end{pmatrix} \begin{pmatrix} H_x \\ H_y \\ H_z \end{pmatrix} \tag{4.1.11}$$

where $\tilde{\chi}$ is the dynamic susceptibility tensor. Notice that for the given configuration the total magnetization can be written as

$$M = M_s + M_{ac} = \begin{pmatrix} M_x \\ M_y \\ M_z \end{pmatrix} = \begin{pmatrix} \chi_{xx} & \chi_{xy} & 0 \\ \chi_{yx} & \chi_{yy} & 0 \\ 0 & 0 & 0 \end{pmatrix} \begin{pmatrix} H_x \\ H_y \\ H_z \end{pmatrix} = \tilde{\chi}(H_0 + H_{ac})$$

where $\chi_0 = \frac{H_0}{M_s}$. Comparing Equation(4.1.11) with Equation(4.1.9) and Equation(4.1.10) the elements of $\tilde{\chi}$ are obtained as

$$\chi_{xx} = \chi_{yy} = \frac{\omega_c \omega_m}{\omega_c^2 - \omega^2}$$

$$\chi_{xy} = \chi_{yx} = -i\frac{\omega \omega_m}{\omega_c^2 - \omega^2}$$

One can now derive the permeability tensor $\tilde{\mu}$ using

$$B = \mu_0(M + H) = \mu_0(1 + \tilde{\chi})H = \tilde{\mu}H$$

The conventional notation for the permeability tensor for a magnetic field bias along the z-dierction is

$$\tilde{\mu} = \begin{pmatrix} \mu_1 & -i\mu_2 & 0 \\ i\mu_2 & \mu_1 & 0 \\ 0 & 0 & \mu_3 \end{pmatrix}$$

where $\mu_1 = \mu_0(1 + \chi_{xx}) = \mu_0(1 + \chi_{yy}) = \mu_0(1 + \frac{\omega\omega_m}{\omega_c^2 - \omega^2})$ and $i\mu_2 = -\mu_0\chi_{xy} = \mu_0\chi_{yx} = i\mu_0\frac{\omega\omega_m}{\omega_c^2 - \omega^2}$[12]. But in our case we use the cgs unit so:

$$\mu_1(\omega) = \mu_{xx} = -\mu_{yy} = 1 - \frac{\omega_c \omega_m}{\omega^2 - \omega_c^2} \tag{4.1.12}$$

$$i\mu_2(\omega) = \mu_{xy} = -\mu_{yx} = i\frac{\omega \omega_m}{\omega^2 - \omega_c^2} \tag{4.1.13}$$

and

$$\mu_3 = \mu_0 = 1 \tag{4.1.14}$$

4.2 Permittivity Tensor of MPFG

The permittivity tensor of the electron-ion plasma is well known with $\vec{B_0}$ directed along the z-axis, the non-zero components of the high frequency permittivity tensor can be

obtained. Consider a plasma in a constant magnetic field $\vec{B}$. From equation of motion of an electron:

$$m\frac{d\vec{V}}{dt} = e\vec{E}_0 e^{-i\omega t} + \frac{e}{c}\vec{V}X\vec{B} \tag{4.2.1}$$

Let $\vec{B}$ parallel to $\hat{z}$

$$m\frac{dv_x}{dt} = eE_{0x}e^{-i\omega t} + \frac{e}{c}v_y B$$
$$m\frac{dv_y}{dt} = eE_{0y}e^{-i\omega t} - \frac{e}{c}v_x B$$
$$m\frac{dv_z}{dt} = eE_{0z}e^{-i\omega t}$$

By doing the above linear equations we can get the velocity components v_x, v_y, and v_z

$$v_x = \frac{e\omega mc^2}{ie^2B^2 - i\omega^2 m^2 c^2}E_x + \frac{e^2Bc}{e^2B^2 - \omega^2 m^2 c^2}E_y$$
$$v_y = \frac{e\omega mc^2}{ie^2B^2 - i\omega^2 m^2 c^2}E_y + \frac{e^2Bc}{e^2B^2 - \omega^2 m^2 c^2}E_x$$
$$v_z = \frac{e}{\omega_m}E_z$$

And from Ohm's law

$$\vec{J} = en\vec{V} = \hat{\sigma}E$$

where $\hat{\sigma}$ is the conductivity tensor.

$$J = \begin{pmatrix} \sigma_{xx} & \sigma_{xy} & \sigma_{xz} \\ \sigma_{yx} & \sigma_{yy} & \sigma_{yz} \\ \sigma_{zx} & \sigma_{zy} & \sigma_{zz} \end{pmatrix} \begin{pmatrix} E_x \\ E_y \\ E_z \end{pmatrix}$$
$$J_x = env_x = \sigma_{xx}E_x = \sigma_{xy}E_y + \sigma_{xz}E_z$$
$$\sigma_{xx} = i\frac{ne^2\omega mc^2}{\omega^2 m^2 c^2 - e^2B^2}, \sigma_{xy} = -\frac{ne^3Bc}{\omega^2 m^2 c^2 - e^2B^2}, \sigma_{xz} = 0$$
$$\sigma_{yy} = i\frac{ne^2\omega mc^2}{\omega^2 m^2 c^2 - e^2B^2}, \sigma_{yx} = \frac{ne^3Bc}{\omega^2 m^2 c^2 - e^2B^2}, \sigma_{yz} = 0$$
$$\sigma_{zz} = i\frac{e^2 n}{\omega m}, \sigma_{zx} = \sigma_{zy} = 0$$

But the permittivity $\varepsilon_{ij} = \delta_{ij} + i\frac{4\pi}{\omega}\sigma_{ij}$ therefore, we can get the permittivity tensors $\varepsilon_{ij}(\omega)$.

$$\varepsilon_1(\omega) = \varepsilon_{xx} = \varepsilon_{yy} = 1 - \frac{\omega_p^2}{\omega^2 - \omega_c^2} \tag{4.2.2}$$

$$i\varepsilon_2(\omega) = \varepsilon_{xy} = -\varepsilon_{yx} = i\frac{\omega_c}{\omega}\frac{\omega_p^2}{\omega^2 - \omega_c^2} \tag{4.2.3}$$

$$\varepsilon_3(\omega) = \varepsilon_{zz} = 1 - \frac{\omega_p^2}{\omega^2} \tag{4.2.4}$$

Where $\omega_p^2 = \frac{4\pi ne^2}{m}$, the electron-ion plasma frequency.

Chapter 5

Refractive Index of MPFG

5.1 Equations of The Refractive Index of MPFG

The Fourier components of the electric and magnetic fields $\vec{E} = \vec{E}(\omega, \vec{k})$ and $\vec{H} = \vec{H}(\omega, \vec{k})$ of plane EMWs having the form $\sim exp[i(\vec{k}\cdot\vec{r} - \omega t)]$ and propagating in MPFG satisfy Equations (2.1.4 and 2.1.5) of Maxwell's equations:

By using Equation (2.1.4) and assuming the cylindrical symmetry of the problem and choosing $\vec{K}$ lie in the X-Z plane:

$$\begin{vmatrix} \hat{i} & \hat{j} & \hat{k} \\ K_x & 0 & K_z \\ E_x & E_y & E_Z \end{vmatrix} = \frac{\omega}{c} \begin{pmatrix} \mu_1 & i\mu_2 & o \\ -i\mu_2 & \mu_1 & 0 \\ 0 & 0 & 1 \end{pmatrix} \begin{pmatrix} H_x \\ H_y \\ H_z \end{pmatrix} \tag{5.1.1}$$

$$\Rightarrow \begin{cases} -K_z E_y = \frac{\omega}{c}(\mu_1 H_x + i\mu_2 H_y) \\ K_z E_x - K_x E_z = \frac{\omega}{c}(-i\mu_2 H_x + \mu_1 H_y) \\ K_x E_y = \frac{\omega}{c} H_z \end{cases} \tag{5.1.2}$$

and from Equation (2.1.5)

$$\begin{vmatrix} \hat{i} & \hat{j} & \hat{k} \\ K_x & 0 & K_z \\ H_x & H_y & H_Z \end{vmatrix} = -\frac{\omega}{c} \begin{pmatrix} \varepsilon_1 & i\varepsilon_2 & o \\ -i\varepsilon_2 & \varepsilon_1 & 0 \\ 0 & 0 & \varepsilon_3 \end{pmatrix} \begin{pmatrix} E_x \\ E_y \\ E_z \end{pmatrix} \tag{5.1.3}$$

Again we will get three more equations is given below.[6, 7, 8]

$$\Rightarrow \begin{cases} -K_z H_y = -\frac{\omega}{c}(\varepsilon_1 E_x + i\varepsilon_2 E_y) \\ K_z H_x - K_x H_z = -\frac{\omega}{c}(-i\varepsilon_2 E_x + \varepsilon_1 E_y) \\ K_x H_y = -\frac{\omega}{c}(\varepsilon_3 E_z) \end{cases} \quad (5.1.4)$$

After eliminating the magnetic field from the systems of Equation (5.1.2) and Equation (5.1.4), we obtain the system of linear algebraic equation for E_x, E_y, E_z.

$$\begin{cases} (i\frac{\omega^2}{c^2 K_z}\mu_1\varepsilon_2)E_x + (\frac{K_x^2}{K_z}\mu_1 + K_z - \frac{\omega^2}{c^2 K_z}\mu_1\varepsilon_1)E_y - \frac{i\omega^2}{c^2 K_x}\mu_2\varepsilon_3 E_z = 0 \\ (\frac{\omega^2}{c^2 K_z}\mu_2\varepsilon_2 - K_z)E_X + (\frac{i\omega^2}{c^2 K_z}\mu_2\varepsilon_1 - i\frac{K_x^2}{K_z}\mu_2)E_y + (K_x - \frac{\omega^2}{c^2 K_x}\mu_1\varepsilon_3)E_z = 0 \\ \frac{\omega}{c}\varepsilon_1 E_x + i\frac{\omega}{c}\varepsilon_2 E_y + \frac{\omega}{c}\frac{K_z}{K_x}\varepsilon_3 E_z = 0 \end{cases} \quad (5.1.5)$$

By obtaining from the condition of vanishing of the determinant of the system of Equation (5.1.5), we can get the following bi quadratic equation with respect to η^2: where $\eta = \frac{kc}{\omega}$ is the refractive index.

$$A\eta^4 + B\eta^2 + C = 0 \quad (5.1.6)$$

where $A = (\varepsilon_1 sin^2\theta + \varepsilon_3 cos^2\theta)(\mu_1 sin^2\theta + cos^2\theta)$

$B = -(\mu_1\Delta_2 + \varepsilon_1\varepsilon_3\Delta_1)sin^2\theta - 2\varepsilon_3(\varepsilon_1\mu_1 + \varepsilon_2\mu_2)cos^2\theta,$

$C = \varepsilon_3\Delta_1\Delta_2$

$\Delta_1 = \mu_1^2 - \mu_2^2$

$\Delta_2 = \varepsilon_1^2 - \varepsilon_2^2$

and θ is the angle between the wave vector $\vec{K}$ and $\vec{H_0}$ The solutions of the bi-quadratic Equation (5.1.6) are

$$\eta_{\pm}^2(\omega, \theta) = \frac{-B \pm \sqrt{B^2 - 4AC}}{2A} \quad (5.1.7)$$

These solutions describe two waves with different refractive indexes propagating in the same direction in MPFG. These are the ordinary η_+ and extraordinary η_- waves, respectively as it is accepted in the theory of CMP[6]

The analysis of the refractive index (Equation (5.1.7)) analytically as a function of frequency for arbitrary direction of propagation of EMWs is rather complex. However, for EMWs propagating parallel and transversal to the magnetic field, one can obtain

simple analytical expressions. For parallel propagation, setting $\theta = 0$ in Equation (5.1.6) and (5.1.7), we get

$$\eta_{\pm}^2(\omega, 0) = \frac{(kc)^2}{\omega^2} = (\varepsilon_1 \pm \varepsilon_2)(\mu_1 \pm \mu_2) \tag{5.1.8}$$

the refractive indexes of the ordinary and extraordinary, circularly polarized EMWs with $E_y = \mp iE_x$ and $E_Z = 0$, propagating along the Z-axis. For waves propagating transversal to $\vec{H_0}$, setting $\theta = \frac{\pi}{2}$, we obtain

$$\eta_{+}^2(\omega, \frac{\pi}{2}) = \frac{(\varepsilon_1^2 - \varepsilon_2^2)}{\varepsilon_1} \tag{5.1.9}$$

and

$$\eta_{-}^2(\omega, \frac{\pi}{2}) = \varepsilon_3 \frac{\mu_1^2 - \mu_2^2}{\mu_1} \tag{5.1.10}$$

The refractive index η_+ relates to the ordinary wave with the electric vector perpendicular to $\vec{H_0}$ and η_- is the refractive index of the extraordinary linearly polarized wave with $E_z \| \vec{H_0}$. These waves propagate along the X-axis.

But the above equations Equations (5.1.8, 5.1.9 and 5.1.10) do not specify the sign of the refractive index of MPFG; it can be plus or minus.

5.2 Negative Refractive Index in MPFG

In order to determine the sign of the refractive index, let us consider the time averaged poynting vector, which is given by

$$\vec{S} = \frac{c}{8\pi} Re(\vec{E} X \vec{H^*}) \tag{5.2.1}$$

and assume that it is positively directed. Simplifying Equation (5.2.1) and expressing the Fourier components of the varying magnetic field through the Fourier components of electric field using Equations (2.1.4 and 2.1.5), we find the non zero components of the poynting vector[6]:

$$S_z^{\pm}(0) = \frac{c}{8\pi} \frac{\eta_{\pm}(0)}{\mu_1 \pm \mu_2} E^2; \; E^2 = |E_x|^2 + |E_y|^2 \qquad S_x^{+} = \frac{c}{8\pi} \eta_{+}(\frac{\pi}{2}) |E_y|^2$$

$$S_x^{-} = \frac{c}{8\pi} \frac{\mu_1 \eta_{-}(\frac{\pi}{2})}{\mu_1^2 \mu_2^2} |E_z|^2 \tag{5.2.2}$$

for waves propagating along and transversal to $\vec{H}_0$, respectively. We see that $\eta_+(\frac{\pi}{2})$ does not depend on the parameters of the magnetic subsystem and is positive when $\frac{(\varepsilon_1^2-\varepsilon_2^2)}{\varepsilon_1} > 1$ as in CMP.

Inspecting the above formulas and keeping in mind that $S_z^{\pm} > 0$ and $S_x^{-} > 0$, we obtain the relations that specify the sign of the refractive index. That is

$$\frac{\eta_{\pm}(0)}{\mu_1 \pm \mu_2} > 0 \quad and \qquad \frac{\mu_1 \eta_-(\frac{\pi}{2})}{\mu_1^2 - \mu_2^2} > 0$$

We can see that the refractive index of the waves propagating along the magnetic field is positive when $\mu_1 \pm \mu_2 > 0$ and $\varepsilon_1 \pm \varepsilon_2 > 0$, simultaneously but it will be negative when $\mu_1 \pm \mu_2 < 0$ and $\varepsilon_1 \pm \varepsilon_2 < 0$,simultaneously[6]. Similarly, the refractive index of the extraordinary wave propagating transversal to the magnetic field is $\eta_-(\frac{\pi}{2}) > 0$ when $\frac{\mu_1}{\mu_1^2-\mu_2^2} > 0$ and $\varepsilon_3 > 0$, and $\eta_-(\frac{\pi}{2}) < 0$ when $\frac{\mu_1}{\mu_1^2-\mu_2^2} < 0$ and $\varepsilon_3 < 0$ [6]. To describe in detail, the dispersion of the components of permittivity and permeability tensors is important at $\omega \to \omega_c$, let us specify the frequency range introducing a dimensionless frequency $x = \frac{\omega-\omega_c}{\omega_c} << 1$. With this in mind, we obtain

$$\mu_1 = 1 - \frac{\alpha_m}{x(x+2)} \quad , \quad \mu_2 = \frac{\alpha_m(x+1)}{x(x+2)} \quad , \quad \varepsilon_1 = 1 - \frac{\alpha_e^2}{x(x+2)}$$

$$\varepsilon_2 = \frac{\alpha_e^2}{x(x+1)(x+2)} \quad , \quad \varepsilon_3 = 1 - \frac{\alpha_e^2}{(x+1)^2} \tag{5.2.3}$$

where $\alpha_e = \frac{\omega_p}{\omega_c}$, $\alpha_m = \frac{\omega_m}{\omega_c}$

Now we can get the refractive index of the waves propagating along the magnetic field in terms of the dimensionless frequency x. Using Equation (5.1.8) and Equation (5.2.3), we obtain

$$\eta_+^2(x,0) = \left(1 - \tfrac{\alpha_e^2}{(x+1)(x+2)}\right)\left(1 + \tfrac{\alpha_m}{x+2}\right) \tag{5.2.4}$$

$$\eta_-^2(x,0) = \left(1 - \frac{\alpha_e^2}{x(x+1)}\right)\left(1 - \frac{\alpha_m}{x}\right) \tag{5.2.5}$$

Because of $\alpha_m << 1$, the simultaneous dispersion of the permeability and permittivity tensors Equation (5.1.8) is important for $|x| \sim \alpha_m << 1$ remembering that ω should not be very close to ω_c, where the cyclotron waves strongly decay in the magnetized plasma.

5.3 Waves Propagating Along The Magnetic Field

From Equation (5.2.4), the ordinary wave propagates along the magnetic field in MPFG for $x \sim \alpha_m << 1$ and $\alpha_e << 1$ that yields $\eta_+^2(x,0) \approx 1 > 0$. The magnetic subsystem does not change the sign of $\eta_+^2(x,0)$. It is controlled by the electrons as in Conventional Magnetized Plasma(CMP)[6].

But when we take the extraordinary wave in CMP($\alpha_m = 0$), the wave only propagates if $x(x+1) > \alpha_e^2$[6].

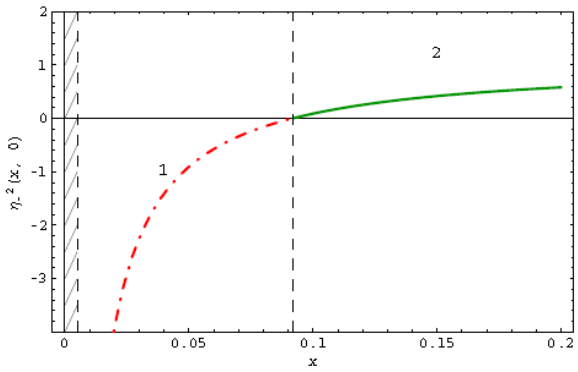

Figure 5.1: The refractive index squared versus the dimensionless frequency (x) of CMP for $\alpha_e^2 = 0.1$.

The above Figure (5.1) shows $\eta_-^2(x,0)$ of CMP versus the dimensionless frequency x for $\alpha_e^2 = 0.1$. The shaded region is related to small frequencies $0 < x \leq 1o^{-4}$, where our theory does not work and requires taking account of the wave damping.

If ferrite grains(ferromagnetic components) are added to CMP, the theory of Veselago, "propagation of waves in left handed media" comes true in MPFG.

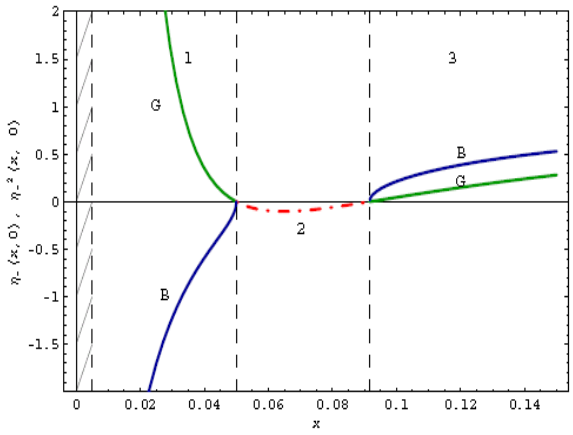

Figure 5.2: The graph of $\eta_-^2(x,0)$ (solid line G) and $\eta_-(x,0)$ (solid line B) of MPFG versus x

In the above Figure (5.2) we showed $\eta_-^2(x,0)$ and $\eta_-(x,0)$ of MPFG versus x. For $x(x+1) \approx x < \alpha_e^2$ and $x < \alpha_m$, MPFG is transparent.

By assuming $\alpha_m < \alpha_e^2$, in the frequency range $\alpha_m < x < \alpha_e^2$ remains nontransparent $(\eta_-^2 < 0)$.

5.4 Refractive Index of Usual and Tuned MPFG

We have seen that the refractive index of the extraordinary EMWs propagating in MPFG parallel to the constant magnetic field, which is directed along the Z-axis is given by Equation (5.1.8).

$$\eta_-^2(\omega,0) = \frac{(kc)^2}{\omega^2} = (\varepsilon_1 - \varepsilon_2)(\mu_1 - \mu_2) \tag{5.4.1}$$

$$\Rightarrow \eta_- = \frac{kc}{\omega} = \sqrt{(\varepsilon_1 - \varepsilon_2)(\mu_1 - \mu_2)} \tag{5.4.2}$$

Note that the frequency of EMWs should not be very close to ω_c (x is not close to zero), where the cyclotron waves in plasma strongly decay.

By substituting $\varepsilon_1, \varepsilon_2, \mu_1$, and μ_2 in terms of the reduced dimensionless frequency in to Equation (5.4.2), we get:

$$\eta(x) = \sqrt{(1 - \frac{\alpha_e^2}{x(x+1)})(1 - \frac{\alpha_m}{x})} \tag{5.4.3}$$

Let us consider $\omega > \omega_c$, i.e the reduced frequency $x > 0$, then the relation between the refractive index of MPFG and the reduced frequency is analyzed in Figure (5.3).

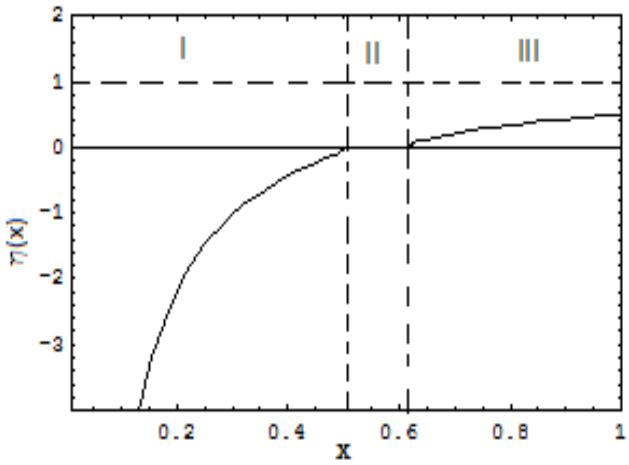

Figure 5.3: The refractive index $\eta(x)$ of the usual MPFG versus x for $\alpha_m = 0.5$ and $\alpha_e^2 = 1$.

We can see that there are three frequency domains. In the first domain(I) the refractive index is negative,$\eta < 0$, and transparent for EMWs. In the second domain (II), η is purely imaginary and nontransparent for EMWs. In the third domain(III), η and approaches to unite for large x. At points where $\eta = 0$, $\frac{d}{dx}\eta \to 0$, the usual MPFG is the system where no relation between α_e and α_m.

By choosing appropriate parameters of the MPFG system, such as the external magnetic field, density number of the electrons and typical size of the ferrite grains, we can obtain the relation[13]:

$$\alpha_e^2 = \alpha_m(1 + \alpha_m) \tag{5.4.4}$$

We call this system the tuned MPFG. The refractive index of the tuned MPFG will be in the following form.

$$\eta_-(x) = (1 - \frac{\alpha_m}{x})\sqrt{1 + \frac{\alpha_m}{1 + x}} \tag{5.4.5}$$

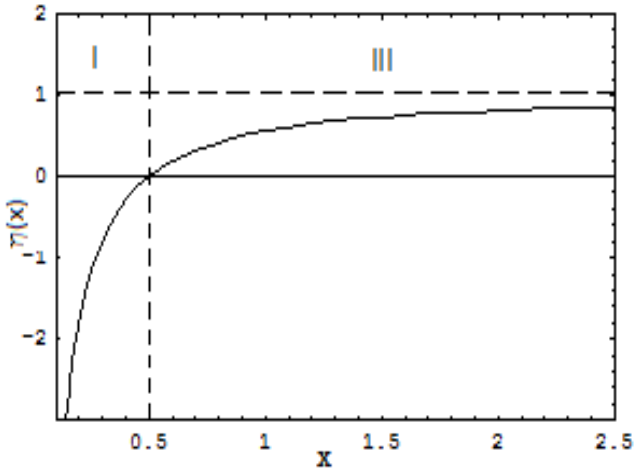

cm

Figure 5.4: The refractive index $\eta(x)$ of the tuned MPFG versus x, for $\alpha_m = 0.5$ and $\alpha_e^2 = 0.75$.

The above Figure (5.4) shows the refractive index $\eta_-(x)$ as a function of the reduced dimensionless frequency x of the tuned MPFG. For frequencies $x < \alpha_m, \eta(x)$ is negative(domain I) and for $x > \alpha_m$ it is positive(domain II). In the tuned MPFG, EMWs will not be attenuated for an entire frequency range $x > 0$. The non transparent region(domain-III) Figure(5.4.1) that exists in the usual MPFG will not longer appear in the tuned MPFG Figure (5.2). Moreover, the function $\frac{d}{dx}\eta_-(x)$ is continuous for all frequencies; unlike that of the usual MPFG[13].

5.5 Phase and Group Velocities of Slow Waves in MPFG

Phase velocity describes the velocity of a peak(crest and troughs) of a wave moves along the direction of propagation. To find the phase velocity, let us consider a point on the sine wave at a particular instant of time, then the wave equation can be written as $Y = Asin\omega t$. After certain time say t_0 if the point is displaced by a distance X the equation is given by:

$$Y = Asin[\omega(t - t_0)]$$

$$Y = Asin[\omega(t - \frac{X}{V})] = Asin[\omega t - KX]$$

where $K = \frac{\omega}{V}$. Therefore, the velocity of individual wave, phase velocity, V_{ph}, will be

$$V_{ph} = \frac{\omega}{k} = \frac{c}{\eta}$$

But in our case, we will take the extraordinary wave propagating along the magnetic field. So the phase velocity will be

$$V_{ph} = \frac{c}{\eta_-(x,0)} = \frac{c}{\sqrt{(1 - \frac{\alpha_e^2}{x(x+1)})(1 - \frac{\alpha_m}{x})}} \tag{5.5.1}$$

As we noticed above, the refractive index of the extraordinary wave propagating along $\vec{H}_0$ is positive when $1 - \frac{\alpha_e^2}{x(x+1)} = \varepsilon_{eff-}(0) > 0$ and $1 - \frac{\alpha_m}{x} = \mu_{eff-}(0) > 0$, and is negative when $\varepsilon_{eff-}(0) < 0$ and $\mu_{eff-}(0) < 0$, simultaneously. Therefore, the phase velocity Equation (5.5.1) is negative in the frequency range, where $\eta_-(x.o) < 0$.

When a group of two or more waves of nearly same frequencies are superimposed on each other, the resultant wave will have different properties from those of the individual waves. So the group velocity will be:

$$\upsilon_g = \frac{d\omega}{dk} = \frac{1}{\frac{dk}{d\omega}}, \qquad k = \frac{\omega\eta}{c}$$

$$\Longrightarrow \upsilon_g = \frac{c}{\eta + \omega\frac{d\eta}{d\omega}}, \qquad d\omega = \omega_c dx, \quad \omega = \omega_c(x+1)$$

$$\Longrightarrow \upsilon_g = \frac{c}{\eta(x) + (x+1)\frac{d\eta(x)}{dx}}$$

$$\Longrightarrow \upsilon_g = \frac{c\eta(x)}{(\eta(x))^2 + \frac{(x+1)}{2}[(\frac{x-\alpha_m}{x})(\frac{2x\alpha_e^2+\alpha_e^2}{x^2(x+1)^2}) + (\frac{x(x+1)-\alpha_e^2}{x(x+1)})(\frac{\alpha_m}{x^2})]}$$

$$\upsilon_g(x) = \frac{cx^2\sqrt{(x+1)(x-\alpha_m)(x^2+x-\alpha_e^2)}}{x^4 + (1-\frac{\alpha_m}{2})x^3 + \frac{1}{2}(\alpha_m + \alpha_e^2 - \alpha_m\alpha_e^2)x - \alpha_m\alpha_e^2} \tag{5.5.2}$$

The dependence of the normalized group velocity, $\frac{\upsilon_g}{c}$, versus the reduced frequency, x, is shown in Figure(5.5) below.

One can see that for the frequency range where $\eta < 0$, the maximum of the normalized group velocity $\frac{\upsilon_g}{c}$ approximately equals to 0.02 which is much less than the speed of light.

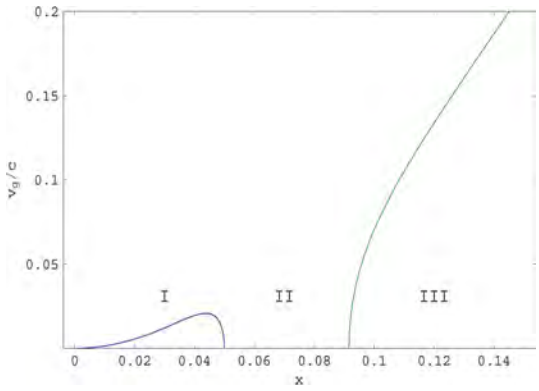

Figure 5.5: The group velocity normalized with respect to the speed of light $\frac{\upsilon_g}{c}$ of the usual MPFG versus the reduced frequency x, for $\alpha_m = 0.05$ and $\alpha_e^2 = 0.1$. For large $x, \upsilon_g \to 1$ (not shown in the graph).

For relatively large parameters $\alpha_m = 1.5$ and $\alpha_e^2 = 2$, as the above Figure (5.5) shows the maximum of $\frac{\upsilon_g}{c} \approx 0.25 < 1$.[13]

The group velocity in the tuned MPFG using Equation (5.5.2) with account Equation (5.4.4) will be

$$\upsilon_g(x) = \frac{cx^2\sqrt{(x+1)(x+\alpha_m+1)}}{x^3 + (1+\frac{\alpha_m}{2})x^2 + \alpha_m(1+\frac{\alpha_m}{2})x + \alpha_m(1+\alpha_m)} \tag{5.5.3}$$

For an arbitrarily value of $\alpha_m = 0.05$, by using Equation (5.4.4), the tuned value of α_e^2 will be 0.0525. If we choose $\alpha_e^2 \neq 0.0525$ for $\alpha_m = 0.05$, the non transparent region will also appear like the usual MPFG. But when we choose α_e^2 much closer to 0.0525 the non transparent region becomes much narrowed. In Figure (5.6) we have showed how the non transparent region becomes narrow when the value of α_e^2 approaches to the tuned value, 0.0525.

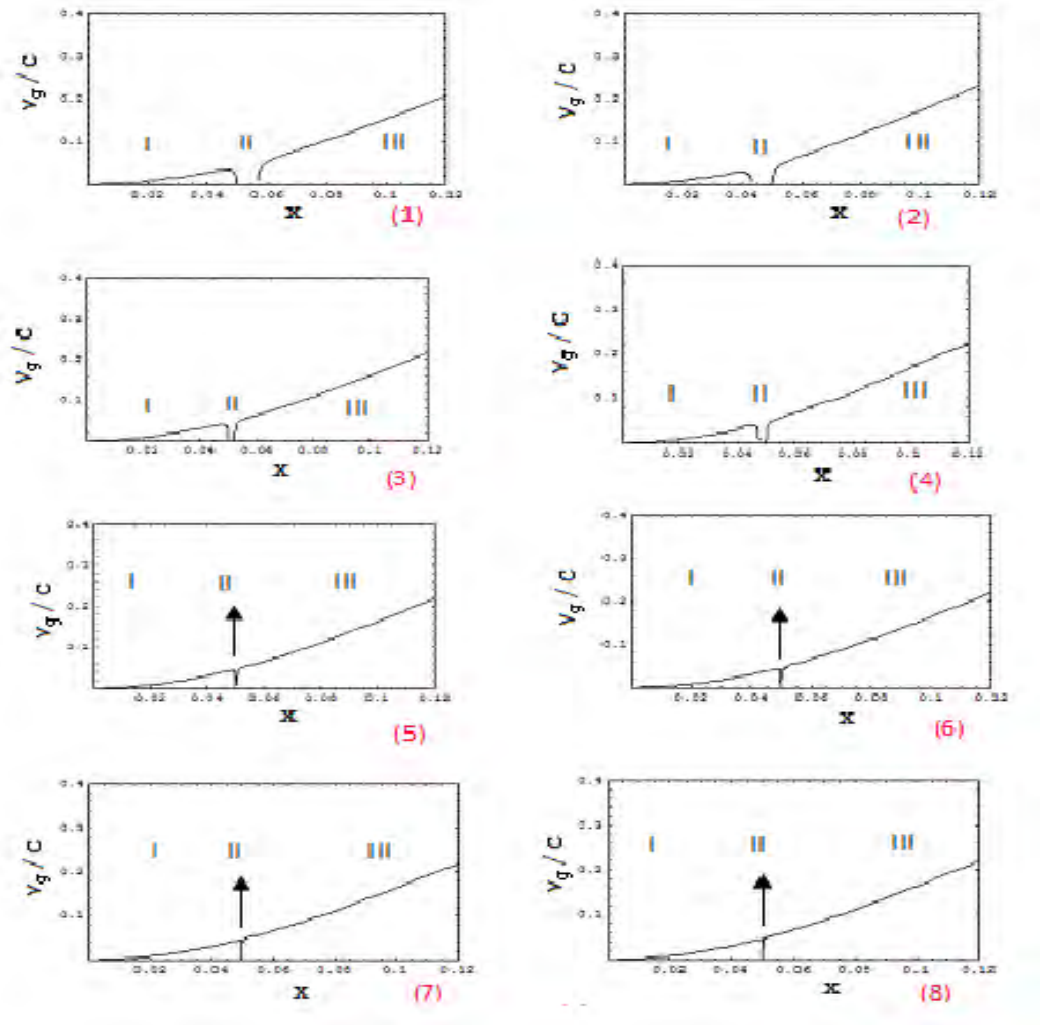

Figure 5.6: The group velocity normalized with respect to the speed of $\frac{v_g}{c}$ of the usual MPFG versus different reduced frequencies x. For $\alpha_m = 0.05$ the corresponding α_e^2 values of each grpahs are
$0.06(1), 0.045(2), 0.055(3), 0.050(4), 0.053(5), 0.053(6), 0.0527(7)$, and $0.0523(8)$.

Finally the normalized group velocity, $\frac{v_g}{c}$, versus the reduced frequency, x, for the tuned MPFG is given by in Figure (5.7).

When we take $x \to \infty$ for the above Equations (5.5.2)and (5.5.3), the normalized group velocity$\frac{v_g}{c}$ will be:

$$\lim_{x\to\infty} \frac{x^2\sqrt{(x+1)(x-\alpha_m)(x^2+x-\alpha_e^2)}}{x^4+(1-\frac{\alpha_m}{2})+\frac{1}{2}(\alpha_m+\alpha_e^2-\alpha_m\alpha_e^2)-\alpha_m\alpha_e^2} = 1$$

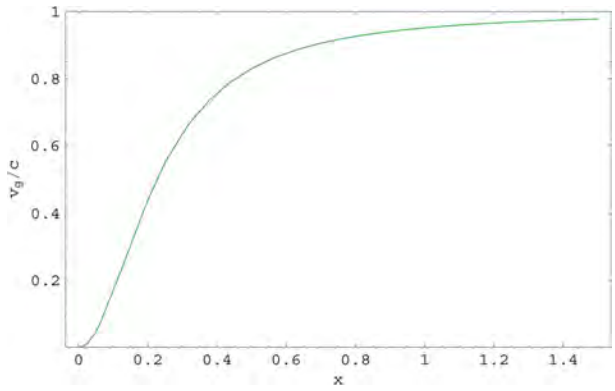

Figure 5.7: The group velocity normalized with respect to the speed of light $\frac{\upsilon_g}{c}$ of the tuned MPFG versus the reduced frequency for $\alpha_m = 0.05$.

Therefore, the group velocity approximately equal to the speed of light for very large frequency, $x \to \infty$ and the next section will figure out what the normalized group velocity looks like with different values of α_m and α_e^2.

5.6 Group Velocity With Different Frequencies α_m and α_e^2 in MPFG

In the previous section, we calculated the normalized group velocity $\frac{\upsilon_g}{c}$ in terms of the reduced frequency x. Now, we tried to find the maximum value of the group velocity $\upsilon_g(x)$ of the usual MPFG in different frequency ranges where $\eta(x) < 0$. For our case we arbitrarily choose $\alpha_m = 0.005, 0.5, 1$ and the corresponding $\alpha_e^2 = 0.01, 1, 2.1$, and 3.

From the three graphs Figure $(5.8, 5.9, 5.10,)$, we can see that, it is possible to find the maximum group velocity $\upsilon_g(x)$ which is in the frequency range where the negative refraction appears. Also we can conclude that the group velocity starts with slower velocity than the speed of light around the ends of the non transparent boundary region. Finally, when we select the value of α_m and α_e^2 according to the relation $\alpha_e^2 = \alpha_m(1+\alpha_m)$, the non transparent region become more narrowed, Otherwise the region become wide.

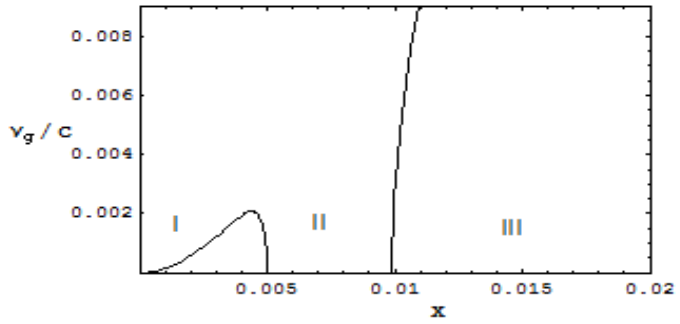

Figure 5.8: The group velocity normalized with respect to the speed of light $\frac{v_g}{c}$ of the usual MPFG versus the reduced frequency, for $\alpha_m = 0.005$ and $\alpha_e^2 = 0.01$. Maximum value of the group velocity in the frequency range where $\eta < 0$ is 0.002.

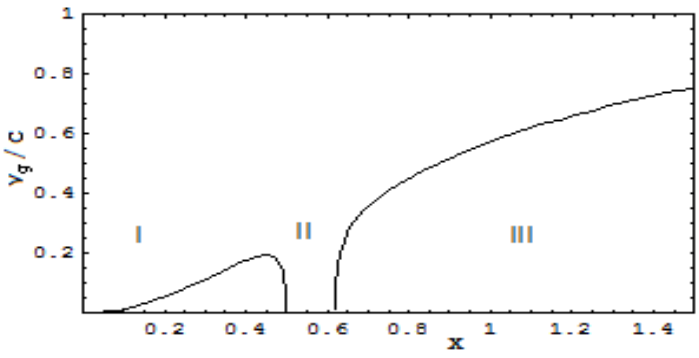

Figure 5.9: The group velocity normalized with respect to the speed of light $\frac{v_g}{c}$ of the usual MPFG versus the reduced frequency, for $\alpha_m = 0.5$ and $\alpha_e^2 = 1$. Maximum value of the group velocity in the frequency range where $\eta < 0$ is 0.2.

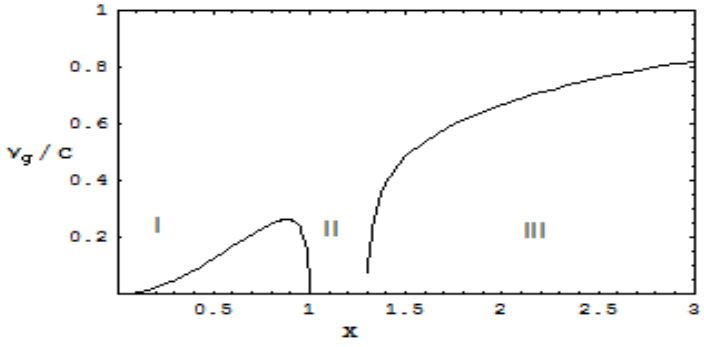

Figure 5.10: The group velocity normalized with respect to the speed of light $\frac{v_g}{c}$ of the usual MPFG versus the reduced frequency, for $\alpha_m = 1$ and $\alpha_e^2 = 3$. Maximum value of the group velocity in the frequency range where $\eta < 0$ is approximately 0.3.

Chapter 6

Conclusion

The aim of this thesis was to understand the physics of metamaterials and describe different experimental realizations to configure this left-handed media. Also we specially focused on how the medium of Magnetized plasma with Ferromagnetic Grains (MPFG) manifests the properties of left-handed medium in a narrow frequency band around the cyclotron frequency ω_c.

We studied the building blocks of metamaterials. Those are an array of thin metallic wires, to produce negative permittivity and split-ring resonator (SRR) which exhibits a negative permeability regime in the vicinity of a magnetic resonance frequency. For MPFG system the dispersion properties are managed by the permittivity and permeability tensors. As some researchers showed that the conventional magnetized plasma is not transparent in the vicinity of ω_c. But when we add ferromagnetic grains in this conventional magnetized plasma the medium becomes transparent for EMWs around that frequency.

Around ω_c, we have shown that the extraordinary wave propagating along and transversal to the external magnetic field both refractive index and phase velocity have negative value. But the group velocity of this wave is always positive. Finally, the interesting finding of this thesis is that the maximum value of the group velocity $v_g(x)$ for the usual MPFG with typical parameters ($\alpha_m << 1$) in the frequency ranges where $\eta(x) < 0$ is much smaller than velocity of light.

Reference

[1] L. I. Mandel'stam, JETP **15**, 465 (1949) (in Russian).

[2] D.V. Sivukhin, The energy of electromagnetic waves in dispersive media, Opt. Spek trosk., **3**, pp. 308-312, 1957.

[3] V.G. Veselago, The electrodynamics of substances with simultaneously negative val ues of permittivity and permeability, Sov. Phys. Uspekhi, **10**, p.509, 1968.

[4] D.R. Smith, N. Kroll, Negative Refractive Index in Left-Handed Materials, Phys. Rev. Lett., **85**, Number 14, 2000.

[5] J.B. Pendry, A.J. Holden, D.J. Robbins, W.J. Stewart, Magnetism from Conduc tors and Enhanced Nonlinear Phenomena, IEEE Trans. Microwave Theory Tech., **47**, p.2075, 1999.

[6] Belayneh Mesfin,V.N.Mal'nev,E.V.Martysh,Yu.G.Rapoport,Waves and negative re fraction in magnetized plasma with ferritie grains, Phys.Plasmas **17**, 112109 (2010)

[7] V.N.Mal'nev, et al, Ukrainian journal of physics, **52**, No.9, p848 (2007).

[8] V.N.Mal'nev, et al, Ukrainian journal of physics, **53**, No.8, p775 (2008)

[9] V. Veselago, L. Braginsky. V. Shklover C. Hafner, J. Comput. Theor. Nanosci, **3**, No. 2, 2006.

[10] Shelby R A, D. R. Smith and S. Schultz Science **292**, 77 (2001).

[11] $\ddot{U}.\ddot{O}zg\ddot{u}r$, Y. Alivov, H. Morcoc, Microwave Ferrites, Part 1 Richmond VA 23284 (2009).

[12] L. D. Landau, E. M. Lifshits, and L. P. Pitaevskii, Electrodynamics of Continuous Media (Butterworth-Heinemann.Oxford, 1984).

[13] Belayneh Mesfin,V.N.Mal'nev, Slow Packets of EMWs in magnetized plasma with ferritie grains, Phys.Plasmas **19**, 032101 (2012).

Declaration

This thesis is my original work, has not been presented for a degree in any other University and that all the sources of material used for the thesis have been dully acknowledged.

Name:Markos Mehretie

Signature:– – – – – – – – – – –

Place and time of submission: Addis Ababa University , June 2012

This thesis has been submitted for examination with my approval as University advisor.

Name:Prof.V.N.Mal'nev

Signature:– – – – – – – – – ––